

Strong hemispheric coupling of glacial climate through freshwater discharge and ocean circulation

R. Knutti¹, J. Flückiger¹, T. F. Stocker¹ & A. Timmermann²

¹Climate and Environmental Physics, Physics Institute, University of Bern, Sidlerstrasse 5, CH-3012 Bern, Switzerland

²IFM-GEOMAR, Leibniz-Institut für Meereswissenschaften, Düsternbrooker Weg 20, D-24105 Kiel, Germany

The climate of the last glacial period was extremely variable, characterized by abrupt warming events in the Northern Hemisphere, accompanied by slower temperature changes in Antarctica and variations of global sea level. It is generally accepted that this millennial-scale climate variability was caused by abrupt changes in the ocean thermohaline circulation. Here we use a coupled ocean–atmosphere–sea ice model to show that freshwater discharge into the North Atlantic Ocean, in addition to a reduction of the thermohaline circulation, has a direct effect on Southern Ocean temperature. The related anomalous oceanic southward heat transport arises from a zonal density gradient in the subtropical North Atlantic caused by a fast wave-adjustment process. We present an extended and quantitative bipolar seesaw concept that explains the timing and amplitude of Greenland and Antarctic temperature changes, the slow changes in Antarctic temperature and its similarity to sea level, as well as a possible time lag of sea level with respect to Antarctic temperature during Marine Isotope Stage 3.

The climate over much of the last glacial period was extremely variable on a millennial timescale. The North Atlantic climate was punctuated by warm phases recorded in proxies over most of the Northern Hemisphere¹. These so-called Dansgaard–Oeschger (DO) events² were characterized by changes from cold (stadial) towards warmer and wetter (interstadial) conditions, with shifts of up to 16 °C observed within a few decades in Greenland^{3–5}, followed by a more gradual cooling over a few hundred to thousand years. The long-lasting DO events were preceded by massive ice surges from the Northern Hemisphere ice sheets. These so-called Heinrich events are documented as thick layers of ice-rafted debris in marine sediments in the North Atlantic^{6,7}. They coincide with cold conditions in the North Atlantic region, warm episodes in Antarctica⁸ and with increases in sea level of 10 to 35 m (refs 9–12). Although the body of observational data is growing, the physical processes behind these events remain elusive.

Guided by evidence from marine sediments for massive reorganizations of the ocean circulation¹³, and modelling results^{14,15}, a concept known as the ‘thermal bipolar seesaw’ was suggested, in which abrupt changes in the strength of the ocean thermohaline circulation (THC) affect the polar climate through changes in the meridional heat transport^{14,16–20}. The THC is sensitive to the Atlantic freshwater balance and exhibits a threshold and hysteresis behaviour^{21–23}. It was argued that the increased glacial climate variability is a result of different stability properties of the glacial thermohaline circulation as compared to today¹⁹. Although in qualitative agreement with many proxies, important issues remain unclear from the published modelling studies. In particular, most models^{19,24} so far have underestimated either the large temperature shifts of 8 °C and more over Greenland and parts of the North Atlantic region, or the changes of about 3 °C over the Antarctic continent^{25–27}. Furthermore, it is difficult to reconcile the conspicuous temporal relationship between the abrupt shifts in Greenland² and the relatively slow changes in the Antarctic temperature reconstructions²⁸ in a physically consistent way.

Here we present results using the ECBILT-CLIO model^{29,30}, which consists of an ocean general circulation model, coupled to a sea-ice and a simplified dynamical atmosphere model. This coupled global atmosphere–ocean model (CGAOM) is forced by meltwater

discharge into the North Atlantic (see Methods). On the basis of the simulated climate events, we propose a mechanism by which freshwater discharge into the Northern Hemisphere directly affects the Southern Ocean temperature through two distinct, but intimately related, ocean circulation feedbacks. This concept, combined with a multi-millennial transient climate model simulation of abrupt climate events, provides a consistent framework to answer a number of open questions that have remained unresolved until now. This includes the timing, amplitude and spatial extent of DO and Heinrich events, the slow timescale associated with Antarctic warm phases, the similarity and lag of sea level to southern temperature and the source of the meltwater discharge.

The climate effect of freshwater discharge

To investigate the processes relating northern and southern high-latitude temperatures, three model simulations using idealized freshwater discharge scenarios are shown in Fig. 1. For case A, the freshwater discharge into the North Atlantic leads to a partial shutdown of the deepwater formation and a cooling in the North Atlantic region. The subsequent recovery to warm conditions coincides approximately with the cooling in the Southern Ocean region. For both cases B and C, the freshwater discharge is sufficient to stop the meridional overturning completely, causing a cooling in the north and a warming in the south. While the cooling in the North Atlantic has a similar magnitude in cases B and C, the Southern Ocean warming is larger for a larger freshwater input. This is in contradiction with the classical ‘thermal bipolar seesaw’ picture, in which southern temperature is determined by northern temperature only²⁰. In addition, southern temperature in case C starts to decrease several centuries before the onset of northern temperature increase. The similarity of southern temperature time series with the freshwater forcing in the North Atlantic is also simulated for different scenarios (not shown) and thus suggests a direct process by which northern freshwater discharge affects southern temperature.

To elucidate the physics of this process, equilibrium simulations using a sustained freshwater input into the North Atlantic of zero, 0.5 and 1.0 Sv (control, F0.5 and F1.0, respectively; 1 Sv = 10⁶ m³ s⁻¹) were performed. Figure 2a shows the simulated

temperature anomaly pattern in the Atlantic arising from the complete collapse of the meridional overturning simulated for F0.5. The surface North Atlantic and the deep Atlantic cool by several degrees, while the South Atlantic and Southern Ocean warm in the upper 1,500 m, consistent with previous model studies^{31–33}. A subsurface warming is seen north of about 60° N, caused by the cessation of deep convective mixing of cold surface water, in particular north of Iceland. Because fresh water affects both the THC and southern temperature as long as the THC is active, the effect of fresh water is best isolated when comparing the two states F0.5 and F1.0 in which the THC is collapsed. The additional freshwater discharge in F1.0 leads to an anomalous southward mass transport of about 2 Sv in the Atlantic south of 40° N, compensated by a return flow between 500 and 1,500 m in depth (Fig. 2b). This causes an anomalous southward heat transport of 0.1 PW, which warms the Southern Ocean sea surface temperature by about 1.5 °C. Although the subsurface Atlantic cools between 20° S and 40° N and warms north of 40° N, this is barely seen at the surface, probably owing to the strong stratification arising from the freshwater cap.

The anomalous meridional transport is due to a zonal density gradient caused by the freshwater input in the following way. The density changes associated with the North Atlantic fresh water trigger Kelvin waves, which propagate along the western Atlantic coast towards the Equator³⁴. Owing to the Coriolis effect, they are forced to travel along the Equator towards the coast of Africa, where they split into a northern and southern branch. While moving poleward, they radiate Rossby waves, which readjust the interior transport of the North and South Atlantic. Overall, our simulated global thermocline anomaly pattern (not shown) is consistent with this wave-adjustment mechanism^{34,35}. Rossby waves establish large-scale pressure (sea level) gradients that are accompanied by geostrophic flow anomalies (see Fig. 2c). North of the Equator these southward geostrophic currents are relatively strong, owing to the weakness of the Coriolis force and the presence of large sea-level gradients in the western boundary region. Cross-equatorial mass

transport is possible, because the velocity anomalies occur close to the western boundary of the basin, where friction is important. Finally, a southward cross-equatorial heat transport of about 0.1 PW is established, in response to the North Atlantic freshwater flux anomalies. Typical response times are of the order of one or two decades³⁶. These conclusions are corroborated by an analysis of the

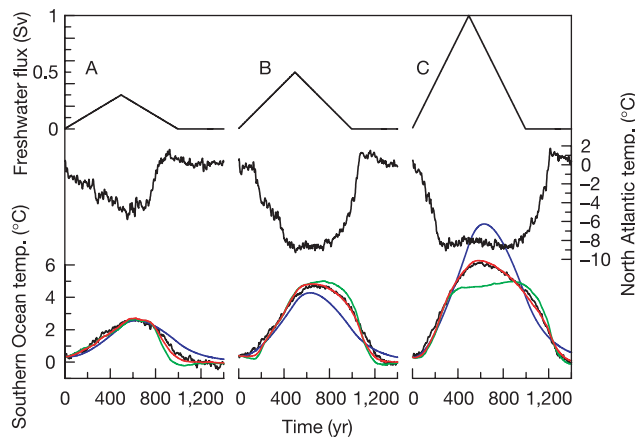


Figure 1 Temperature response to three scenarios of freshwater discharge into the North Atlantic. Freshwater discharge (top), 10-yr running mean of near-surface air temperature of the North Atlantic region (60° W–20° E, 50° N–80° N) (middle) and the Southern Ocean region (65° S–50° S) (bottom) are shown in black. The fresh water causes a partial shutdown of the THC in case A, and a complete shutdown in cases B and C. The classical thermal bipolar seesaw²⁰ (green) predicts the same amplitude of the southern warming for cases B and C and fails to explain the early cooling in southern temperatures. The extended thermal–freshwater seesaw concept (red) correctly predicts both an additional southern warming for case C that is related to the large freshwater input, and the slow southern temperature changes due to slow freshwater changes. The fit here explains more than 98% (r^2) of the southern temperature response simulated by the CGAOM. Fresh water alone (blue) is insufficient to explain the model response.

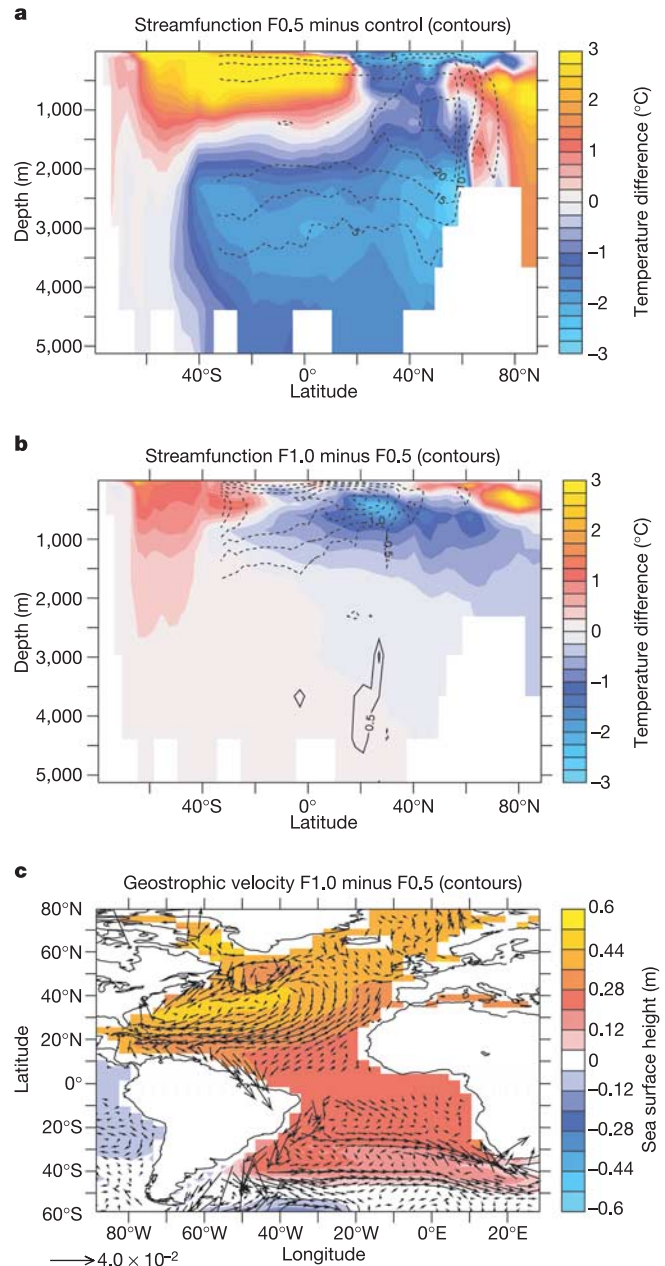


Figure 2 The ocean response to freshwater discharge into the North Atlantic. F1.0 and F0.5 denote 1.0 Sv and 0.5 Sv sustained freshwater discharge, respectively. **a**, The equilibrium Atlantic temperature difference (°C, colours) and meridional streamfunction difference (Sv, contours) resulting from 0.5 Sv freshwater input and the subsequent complete shutdown of the THC. **b**, Doubling the freshwater input leads to an additional temperature and streamfunction anomaly. **c**, Freshwater anomalies trigger a redistribution of the sea surface height (m, colours), owing to fast wave adjustment processes, which in turn drives geostrophic transport anomalies (m s^{-1} , vectors). Subsequently a cross-equatorial anomalous meridional transport is established (contours, **b**), which leads to an export of heat into the Southern Ocean of about 0.1 PW, thereby warming the upper 800 m of the Southern Ocean. On the other hand, associated surface temperature signals in the North Atlantic are weak.

thermal wind balance, as deduced from the upper-ocean zonal density gradients. The ocean adjustment scales linearly with the freshwater perturbation. The freshwater amplitudes in Fig. 2 are only chosen to be large to separate the related signal better from the internal ocean variability.

From these idealized simulations we conclude that the Southern Ocean surface temperature changes are not only determined by the heat transport of the large-scale THC, but are also directly affected by the anomalous meridional overturning circulation (Fig. 2b), which is established in response to the freshwater input in the North Atlantic. This provides a consistent explanation for the apparent but so far unexplained similarity between sea level variations and southern temperatures. Additional model simulations show that the same mechanism works equally well for freshwater input into the North Pacific, whereas it does not operate for freshwater input in the Southern Ocean, where zonal density anomalies cannot be established.

The thermal–freshwater seesaw

The direct effect of freshwater release on the meridional heat flux in the South Atlantic suggests a modification of the thermal bipolar seesaw concept²⁰. Assuming that the Southern Ocean acts like a heat reservoir, we propose the following approximation relating the freshwater flux F and the temperature anomalies T_N , T_S of the

northern and southern region relative to equilibrium climate:

$$d(T_S)/dt = (-aT_N + bF - T_S)/\tau \quad (1)$$

where τ is a typical thermal response timescale of the southern heat reservoir. In this concept, the southern reservoir temperature is controlled by the sum of a meridional oceanic heat transport due to the thermohaline circulation that is assumed to be proportional to $(-\alpha T_N - T_S)$ (ref. 20), and an oceanic heat transport that is proportional to $(\beta F - T_S)$, related to the freshwater input into the North Atlantic.

The three parameters in equation (1) are now determined by a series of transient simulations using the CGAOM (see Methods) in which the circulation is perturbed by a range of different freshwater discharges. The best fit yields a timescale τ of 114 yr; values for a and b are given in the Methods section. This timescale is considerably shorter than the one determined for the original thermal bipolar seesaw fitted to observations²⁰, which was of the order of 1,000 yr. In contrast, our new thermal–freshwater seesaw is based solely on the comprehensive CGAOM, and its agreement with palaeoclimatic proxy data provides an independent check of its validity. The extended thermal–freshwater seesaw concept is able to explain the timing and amplitude of the southern temperature response in the CGAOM in Fig. 1 with very high accuracy. We find that large changes in the freshwater discharge F contribute up to one-third to the amplitude of the southern temperature response T_S , and that the timescale τ is consistent with a thermal inertia timescale of the upper 1,000 m of the Southern Ocean.

An illustrative sequence of climate events

Forcing the CGAOM by freshwater discharge into the North Atlantic in a transient multi-millennial simulation reveals a picture of abrupt climate events that resolves a number of questions that emerged from earlier modelling studies. The illustrative freshwater scenario assumed in Fig. 3 causes large and abrupt changes in the North Atlantic deepwater formation and thus also in the air temperature of the North Atlantic region and Greenland with a magnitude of more than 15 °C in the convection regions. Changes in the modelled Antarctic temperature are up to about 5 °C and are controlled both by the temperature in the North Atlantic and by the amount of fresh water. Recent proxy estimates suggest changes in Antarctic temperature during the glacial of 2 to 4 °C (refs 25–27). This indicates that the peak of northern freshwater input mimicking a Heinrich surge, although intentionally chosen large here to illustrate its effect, is probably at the upper limit. The resulting sea level change of 30 m also suggests that the freshwater amplitude, although consistent with the largest estimate of sea level variations¹², is chosen rather high. The apparent lead of the peak Antarctic warming to the Greenland transition T2 depends on the shape of the freshwater discharge and would be smaller if fresh water was decreased more rapidly. Using the illustrative freshwater scenarios, the CGAOM simulates two types of events in the North Atlantic, a transition from a weak to a strong meridional overturning state (transition T1 in Fig. 3) and a transition from a stratified Atlantic without deepwater formation to a strong overturning state (transition T2). The spatial patterns (shown in Fig. 4) of temperature and precipitation changes of transition T2 suggest that climate changes following a Heinrich event were large in amplitude and seen in most regions of the globe. The qualitative model response is consistent with proxy reconstructions indicating broad cooling of the Southern Hemisphere and warming of the Northern Hemisphere during interstadial phases¹ and, for example, higher accumulation in Greenland, warmer and wetter conditions in Europe³⁷, wet conditions in most of northern subtropical Asia³⁸ and Arabia³⁹, as well as increased rainfall over the Cariaco basin⁴⁰. Many proxies distant from the North Atlantic record the large DO events following a Heinrich event (for example, DO events 8, 12) but not all of the smaller ones (for example, DO events 9, 13)⁴⁰. This is qualitatively

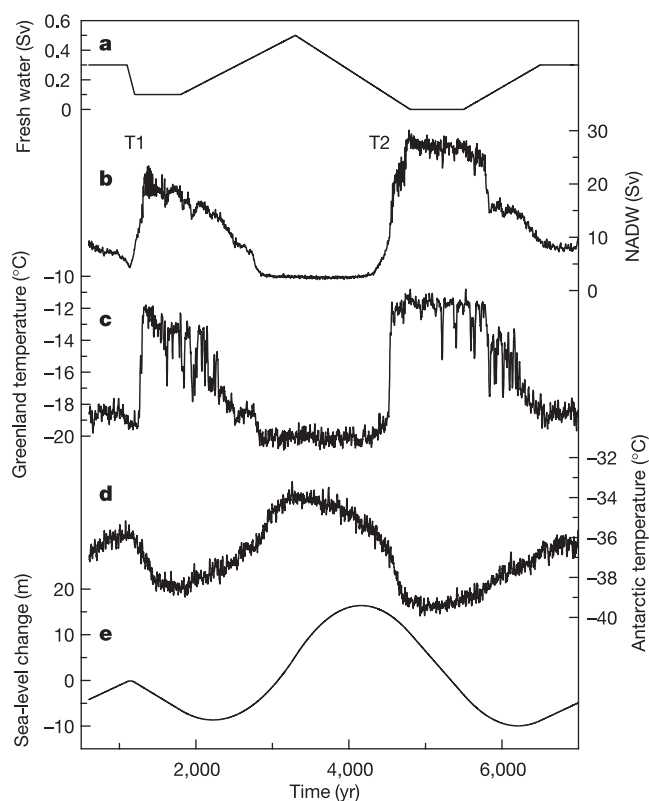


Figure 3 Time evolution of the THC and global sea level and corresponding changes in polar near-surface air temperature in an illustrative scenario of freshwater discharge into the North Atlantic. The fresh water (a) causes abrupt shifts in the North Atlantic deepwater formation (b). The associated massive and abrupt warming events simulated over Greenland (c) and the North Atlantic region are reminiscent of the DO events observed in palaeorecords from the last glacial epoch. Antarctic temperature (d) is influenced by the THC and directly by the freshwater discharge into the North Atlantic. This explains why changes in sea level (e, detrended integral of freshwater input) resemble but lag notably Antarctic temperature, consistent with the proxy reconstructions. Freshwater discharge in this scenario integrates to 30 m sea-level change, the upper limit of published values.

supported here by the smaller amplitude and spatial extent for transition T1 compared to T2. The modelled temperature shift in Greenland is similar for both transitions, also in good agreement with Greenland isotopic records²⁸, which indicate large temperature shifts even for the short DO events. The model response is in line with most proxies showing a hemispheric antiphase temperature pattern¹, and does not support in-phase changes in Greenland and Antarctica^{41,42}.

It is clear from Fig. 3 and from our thermal–freshwater seesaw that the shape of the sea level variations is similar to Antarctic temperature, as recently suggested from a reconstruction of sea level from the Red Sea¹². A significant amount of ice surges must therefore have emerged from the Northern Hemisphere, in line with the generally accepted pattern of the Heinrich surges recorded in the North Atlantic⁷. The results presented here do not preclude contributions to sea level from other locations⁴³. However, additional CGAOM simulations show that freshwater discharge into the North Pacific or into the Gulf of Mexico have a similar effect of warming Antarctica, whereas freshwater discharge from Antarctica has the opposite effect of cooling the Southern Ocean and Antarctica and warming the North Atlantic⁴⁴. Therefore, a dominant contribution from the Antarctic ice sheet to the sea level variations recorded during MIS 3 (refs 9–12) can be excluded.

We find that despite their similarity, sea level in the model lags Antarctic temperature by several centuries. Such a lag can be identified in palaeodata using the benthic oxygen isotope record from a sediment core off Portugal⁹, if taken as a proxy for sea level, and the Byrd oxygen isotope record²⁸ as a proxy for Antarctic temperature (see Fig. 5). Both records are independently synchro-

nized to the GRIP record from Greenland^{8,9}. Maximizing lag correlation in a moving window of 10 kyr suggests a lag of 300 to 1,500 yr of the benthic sea level curve to Antarctic temperature when using the published timescales. However, the uncertainties in the timescales (resolution of the records, gas age–ice age and synchronization uncertainties) and the fact that part of the benthic signal could be caused by changes in ocean temperature (which need not necessarily be in phase with sea level) prevent us from firmly concluding that there is a sea-level lag from the data alone. Equation (1) suggests almost no sea-level lag for changes in the freshwater flux F on short timescales (decades), but a phase lag of up to 90°, equivalent to about 1,000 yr, when assuming changes in F on timescales of a few millennia.

The sequence of events during MIS 3

The sequence of events shown in Fig. 3 is reminiscent of parts of the last glacial period, for example, the time around 45,000 yr before present (45 kyr before present, BP) with DO events 13 and 12. But the complexity of the CGAOM, the uncertainties in the hysteresis behaviour of the glacial thermohaline circulation and the computational cost of the model prevent us from simulating longer time periods. However, equation (1) has been shown to adequately relate the polar temperature anomalies simulated by the CGAOM and can thus be used as a substitute. Here we use the substitute conceptual model to quantify the extent to which the thermal–freshwater seesaw concept can explain the evolution of Greenland and Antarctic temperature reconstructions, as well as sea-level variations during Marine Isotope Stage (MIS) 3. We start from a random time evolution of the freshwater flux F . Subsequently, F is iteratively

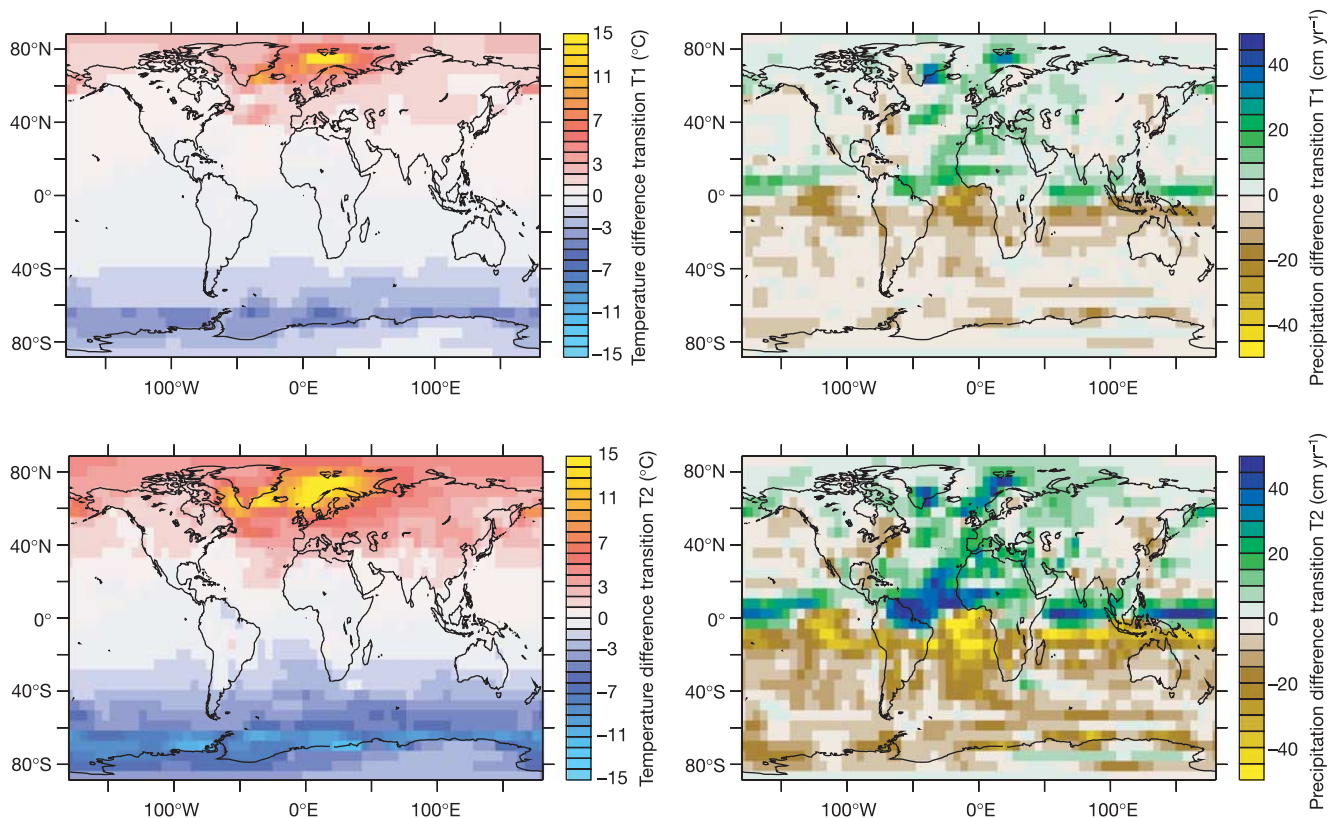


Figure 4 Temperature and precipitation changes simulated for two stadial–interstadial transitions. Transition T1 (shown in Fig. 3) is from a partial ‘off’ to a THC ‘on’ state, transition T2 from a completely collapsed THC state to a strong THC ‘on’ state. The CGAOM predicts that temperature changes were prominent in Greenland for both transitions, but the amplitude and spatial extent was different over most of the Northern Hemisphere. The maps show the near-surface temperature (°C) and precipitation

difference (cm yr⁻¹) for the cold-to-warm transition T1 (1,500 to 1,700 minus 800 to 1,000 model yr, top) and T2 (4,800 to 5,000 minus 3,400 to 3,600 model yr, bottom). These patterns are in agreement with proxy evidence for the long-lasting DO events following a Heinrich event (T2) and for the shorter DO events, which have a weak or no clear counterpart in the south (T1). The large temperature shifts in some areas of the Southern Ocean during transition T2 are caused by changes in sea-ice extent.

changed so as to maximize the correlation between the simulated time series T_N , T_S and sea-level h (obtained from the time integral of F) with the reconstructed time series GRIP $\delta^{18}\text{O}$, Byrd $\delta^{18}\text{O}$ and the sea-level proxy, respectively. T_N is assumed to be proportional to the strength of the THC. The latter is assumed to depend in a tanh way on the freshwater flux F , an approximation to a very narrow hysteresis. Thus, the expressions for the polar temperatures read $T_N = p \tanh(sF)$ and $d(T_S)/dt = (-aT_N + bF - T_S)/\tau$. Parameters are taken from the CGAOM (see Methods)^{25–27}. The optimized freshwater flux time series F and its relation to the reconstructed and simulated time series are depicted in Fig. 5.

Despite the simplicity of this approach, we find correlations of $r = 0.75$, 0.71 and 0.86 of the calculated curves with GRIP $\delta^{18}\text{O}$, Byrd $\delta^{18}\text{O}$ and the sea-level proxy, respectively. Therefore, this concept explains 60% (r^2) of the variability found in the polar temperature and sea-level reconstructions over MIS 3 (60 to 25 kyr BP). In particular, it shows that the slow changes in F explain the low-frequency timescale found in the Byrd isotopic record. Maximum values in the optimized freshwater flux coincide with high input of ice-rafted debris during Heinrich events⁷ and low values of benthic $\delta^{13}\text{C}$, indicating a reduced ventilation of the North Atlantic Deep Water⁹. Although we show here that both the shape of sea-level variations and marine proxies in the North Atlantic over MIS 3 are broadly consistent with meltwater discharge into the North Atlantic only, we note that this concept does not preclude additional meltwater discharge of smaller magnitude elsewhere. A change in the slope parameter s affects the amplitude needed in F

and can thus change the magnitude (but not the shape) of the sea-level variations by at least a factor of two, without significantly changing the correlation values. The magnitude of these sea-level variations in the last glacial epoch is still debated^{10–12}. The benthic record off Portugal⁹ probably reflects changes in both sea level and ocean temperature. A recent reconstruction of sea level¹² shows a very similar shape, which confirms the time evolution (but not necessarily the magnitude) of sea-level variations. However, this reconstruction does not have sufficient age control to be used in this study.

Substituting either the Byrd record or the Byrd and the sea-level record with red noise time series, the same concept can explain only about 40% (r^2) of the variability. This indicates that, in contrast to recent studies^{45,46}, we show here a strong and statistically significant (>99%) coupling of the hemispheres during the climate variations in MIS 3.

Ocean linkage during abrupt climate change

Using a synthesis of proxy data from the last glacial period and a coupled climate model, we have demonstrated that the main patterns of temperature and sea-level variations recorded in a variety of archives during abrupt glacial climate events can largely be explained by changes in the oceanic heat transport related directly to freshwater discharge and the large-scale thermohaline circulation. This supports the view that the ocean circulation and its potential nonlinear changes play a crucial role in modulating the Earth's climate on global and regional scales. But there is also a strong response of the atmospheric circulation and of precipitation, indicating that atmospheric processes and feedbacks are relevant to transmit the abrupt Atlantic climate signals to other regions⁴⁷. We have obtained a quantitative picture of how the ocean circulation has shaped millennial-scale climate variability during the last glacial period, but are still unable to determine whether atmospheric processes, oceanic thresholds, ice-sheet dynamics, and their coupling or an external forcing acted as the pacemaker of abrupt climate changes. □

Methods

The model used for this study is the global coupled atmosphere–ocean–sea ice model ECBILT-CLIO (version 3.0). The atmosphere is represented by the T21, three-level quasi-geostrophic model ECBILT2 (ref. 29), which contains a full hydrological cycle and explicitly computes synoptic variability associated with weather patterns. The ocean model CLIO³⁰ is a primitive equation, free-surface ocean general circulation model with a resolution of 3×3 degrees and 20 unevenly spaced levels, coupled to a thermodynamic–dynamic sea-ice model. The CGAOM includes realistic topography, bathymetry, a simple representation of land surface processes and a bucket runoff scheme. Given the long timescales investigated here, the model is among the most complex climate models that can be applied to study this type of question at present. The model is freely available from <http://www.knmi.nl/onderzk/CKO/ecbilt.html>. The presented simulations use modern boundary conditions. Changing topography, greenhouse gas concentrations, orbital parameters and albedo values to conditions of the Last Glacial Maximum⁴⁸ show very similar results (see Supplementary Fig. S1). Freshwater discharge into the North Atlantic is between 50°N and 70°N , and is uniformly compensated outside the discharge regions to avoid model drift. The coupled model employs weak freshwater flux corrections. Given the large uncertainties in the freshwater budget of the Atlantic, the zero level in freshwater flux can thus be shifted within a wide range. Such model results are clearly sensitive to the shape of the hysteresis of the THC, which is mainly determined by the equilibrium freshwater budget of the Atlantic, and is often tuned by adjusting runoff masks or prescribing freshwater redistributions (flux corrections). Given the uncertainties associated with the THC hysteresis and the feedbacks, which determine the stability of the THC even under modern boundary conditions⁴⁹, we have chosen not to tune the CGAOM to achieve a certain threshold behaviour. Although the processes studied require a comprehensive general circulation ocean model, our conclusions do not depend on a particular threshold behaviour of the THC.

The parameters a , b and τ of equation (1) were determined by minimizing the sum of the squared deviations for southern temperature of the CGAOM and of equation (1), taking fresh water and northern temperature as an input. Near-surface temperatures of the North Atlantic and Southern Ocean region yield $a = 0.41^\circ\text{C}^\circ\text{C}^{-1}$, $b = 3.6^\circ\text{C}\text{Sv}^{-1}$ and $\tau = 114\text{ yr}$ (used for Fig. 1). Correlation of the CGAOM results (10-yr running means) and the response of equation (1) with optimal parameters exceeds $r = 0.97$ in all cases. For the original thermal bipolar seesaw (equation (1), $b = 0$), the fitting procedure yields $\tau = 90\text{ yr}$.

For the conceptual model used in Fig. 5, all parameters except the slope s are fitted from

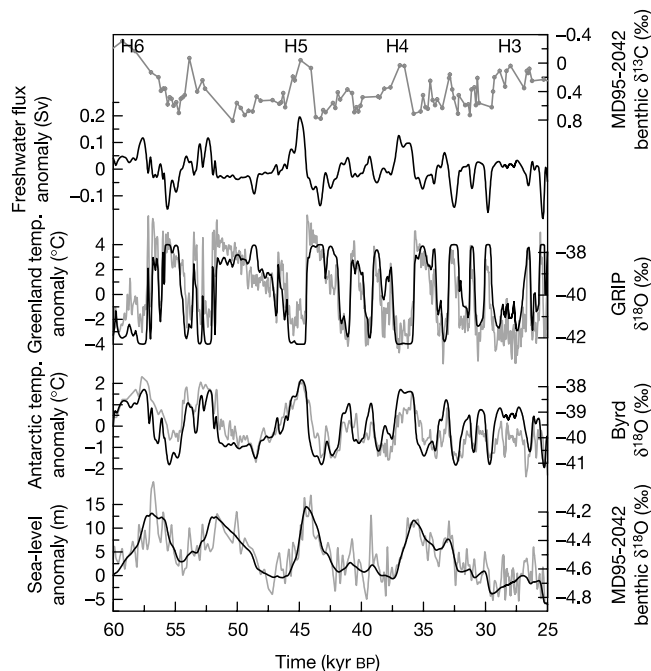


Figure 5 Variability of Greenland and Antarctic temperature and sea-level proxy data (grey, right axes) explained by a conceptual model (black, left axes). The optimized solution to the conceptual model (see text and Methods) shows strong coupling of Greenland and Antarctic temperature, fresh water and sea level during MIS 3 and explains 60% (r^2) of the variability seen in the water isotope reconstructions of GRIP², Byrd²⁸ and the benthic isotope record from off Portugal⁹, which is assumed to be a proxy for sea-level variations. The timing of the optimized freshwater discharge peaks shows remarkable agreement with input of ice-rafted debris during Heinrich events⁷ and low values of benthic $\delta^{13}\text{C}$, indicating reduced ventilation of the North Atlantic Deep Water⁹ (grey, top). Age scales are synchronized to GRIP⁹ and all time series except $\delta^{13}\text{C}$ are splined with a 100-yr cut-off period⁵⁰. Note that benthic $\delta^{13}\text{C}$ and ice-rafted debris are not used to optimize correlation.

the Greenland and Antarctic temperature response of the CGAOM and yield $a = 0.24^{\circ}\text{C}^{\circ}\text{C}^{-1}$, $b = 6.3^{\circ}\text{C Sv}^{-1}$, $\tau = 135\text{ yr}$ and $p = 4^{\circ}\text{C}$. The range of Antarctic temperature variations is required to be in agreement with observations^{25–27}. Models simulating the sensitivity of the THC to fresh water indicate that the range for the slope s is uncertain. However, the choice of the value s is not critical for our conclusion. That only one branch of the THC hysteresis behaviour is captured in our simple model explains why the calculated temperature generally drops too fast at the end of the Antarctic warm event, as compared to reconstructions. Ocean models indicate that the lower branch of the hysteresis ('off-on' transition) is probably more abrupt than the upper one. Such a hysteresis behaviour would temperature a slower decrease in the freshwater flux and thus lead to a slower decrease in Antarctic temperature, while still producing an abrupt warming in Greenland, and thus improve the agreement with proxy data.

Received 1 March; accepted 25 June 2004; doi:10.1038/nature02786.

1. Voelker, A. H. L. & workshop participants. Global distribution of centennial-scale records for Marine Isotope Stage (MIS) 3: A database. *Quat. Sci. Rev.* **21**, 1185–1212 (2002).
2. Dansgaard, W. *et al.* Evidence for general instability of past climate from a 250 kyr ice-core record. *Nature* **364**, 218–220 (1993).
3. Schwander, J. *et al.* Age scale of the air in the summit ice: Implication for glacial-interglacial temperature change. *J. Geophys. Res.* **102**, 19483–19494 (1997).
4. Lang, C., Leuenberger, M., Schwander, J. & Johnsen, S. 16°C rapid temperature variation in central Greenland 70,000 years ago. *Science* **286**, 934–937 (1999).
5. Severinghaus, J. P. & Brook, E. J. Abrupt climate change at the end of the last glacial period inferred from trapped air in polar ice. *Science* **286**, 930–934 (1999).
6. Heinrich, H. Origin and consequences of cyclic ice rafting in the northeast Atlantic Ocean during the past 130,000 years. *Quat. Res.* **29**, 142–152 (1988).
7. Hemming, S. R. Heinrich events: Massive late Pleistocene detritus layers of the North Atlantic and their global climate imprint. *Rev. Geophys.* **42** (2004) doi:10.1029/2003RG000128.
8. Blunier, T. & Brook, E. Timing of millennial-scale climate change in Antarctica and Greenland during the last glacial period. *Science* **291**, 109–112 (2001).
9. Shackleton, N. J., Hall, M. A. & Vincent, E. Phase relationships between millennial scale events 64,000 to 24,000 years ago. *Paleoceanography* **15**, 565–569 (2000).
10. Yokoyama, Y., Esat, T. M. & Lambeck, K. Coupled climate and sea-level changes deduced from Huon Peninsula coral terraces of the last ice age. *Earth Planet. Sci. Lett.* **193**, 579–587 (2001).
11. Chappell, J. Sea level changes forced ice breakouts in the last glacial cycle: New results from coral terraces. *Quat. Sci. Rev.* **21**, 1229–1240 (2002).
12. Siddall, M. *et al.* Sea-level fluctuation during the last glacial cycle. *Nature* **423**, 853–858 (2003).
13. Clark, P. U., Webb, R. S. & Keigwin, L. D. (eds) *Mechanisms of Global Climate Change at Millennial Time Scales* 1–394 (AGU, Washington DC, 1999).
14. Stocker, T. F. & Marchal, O. Abrupt climate change in the computer: Is it real? *Proc. Natl Acad. Sci. USA* **97**, 1362–1365 (2000).
15. Rahmstorf, S. Ocean circulation and climate during the past 120,000 years. *Nature* **419**, 207–214 (2002).
16. Crowley, T. J. North Atlantic deep water cools the southern hemisphere. *Paleoceanography* **7**, 489–497 (1992).
17. Stocker, T. F. The seesaw effect. *Science* **282**, 61–62 (1998).
18. Broecker, W. S. Paleocene circulation during the last deglaciation: A bipolar seesaw? *Paleoceanography* **13**, 119–121 (1998).
19. Ganopolski, A. & Rahmstorf, S. Rapid changes of glacial climate simulated in a coupled climate model. *Nature* **409**, 153–158 (2001).
20. Stocker, T. F. & Johnsen, S. J. A minimum thermodynamic model for the bipolar seesaw. *Paleoceanography* **18**, doi:10.1029/2003PA000920 (2003).
21. Stocker, T. F. & Wright, D. G. Rapid transitions of the ocean's deep circulation induced by changes in surface water fluxes. *Nature* **351**, 729–732 (1991).
22. Mikolajewicz, U. & Maier-Reimer, E. Mixed boundary conditions in ocean general-circulation models and their influence on the stability of the models conveyor belt. *J. Geophys. Res.* **99**, 22633–22644 (1994).
23. Rahmstorf, S. Rapid climate transitions in a coupled ocean-atmosphere model. *Nature* **372**, 82–85 (1994).
24. Schmittner, A., Yoshimori, M. & Weaver, A. J. Instability of glacial climate in a model of the ocean-atmosphere-cryosphere system. *Science* **295**, 1489–1493 (2002).
25. Jouzel, J. *et al.* Magnitude of isotope/temperature scaling for interpretation of central Antarctic ice cores. *J. Geophys. Res.* **108**, doi:10.1029/2003JD002677 (2003).
26. Blunier, T., Schwander, J., Chappellaz, J., Parrenin, F. & Barnola, J.-M. What was the surface temperature in central Antarctica during the last glacial maximum? *Earth Planet. Sci. Lett.* **218**, 379–388 (2004).

27. Stenni, B. *et al.* A late-glacial high-resolution site and source temperature record derived from the EPICA Dome C isotope records (East Antarctica). *Earth Planet. Sci. Lett.* **217**, 183–195 (2003).
28. Johnsen, S. J., Dansgaard, W., Clausen, H. B. & Langway, C. C. Jr Oxygen isotope profiles through the Antarctic and Greenland ice sheets. *Nature* **235**, 429–434 (1972).
29. Opsteegh, J. D., Haarsma, R. J., Selden, F. M. & Kattenberg, A. ECBILT: A dynamic alternative to mixed boundary conditions in ocean models. *Tellus A* **50**, 348–367 (1998).
30. Goosse, H. & Fichefet, T. Importance of ice-ocean interactions for the global ocean circulation: A model study. *J. Geophys. Res.* **104**, 23337–23355 (1999).
31. Stocker, T. F., Wright, D. G. & Broecker, W. S. The influence of high-latitude surface forcing on the global thermohaline circulation. *Paleoceanography* **7**, 529–541 (1992).
32. Schiller, A., Mikolajewicz, U. & Voss, R. The stability of the thermohaline circulation in a coupled ocean-atmosphere general circulation model. *Clim. Dyn.* **13**, 325–348 (1997).
33. Manabe, S. & Stouffer, R. J. Coupled ocean-atmosphere model response to freshwater input: Comparison to Younger Dryas event. *Paleoceanography* **12**, 321–336 (1997).
34. Huang, R. X., Cane, M. A., Naik, N. & Goodman, P. Global adjustment of the thermocline in response to deepwater formation. *Geophys. Res. Lett.* **27**, 759–762 (2000).
35. Hsieh, W., Davey, M. K. & Wajsiwicz, C. The free Kelvin wave in finite-difference models. *J. Phys. Oceanogr.* **13**, 1383–1397 (1983).
36. Johnson, H. & Marshall, D. P. A theory for the surface Atlantic response to thermohaline variability. *J. Phys. Oceanogr.* **32**, 1121–1132 (2002).
37. Allen, J. R. M. *et al.* Rapid environmental changes in southern Europe during the last glacial period. *Nature* **400**, 740–743 (1999).
38. Wang, Y. J. *et al.* A high-resolution absolute-dated late Pleistocene monsoon record from Hulu Cave, China. *Science* **294**, 2345–2348 (2001).
39. Burns, S. J., Fleitmann, D., Matter, A., Kramers, J. & Al-Subbary, A. A. Indian ocean climate and an absolute chronology over Dansgaard/Oeschger events 9 to 13. *Science* **301**, 1365–1367 (2003).
40. Peterson, L. C., Haug, G. H., Hughen, K. A. & Röhl, U. Rapid changes in the hydrologic cycle of the tropical Atlantic during the last glacial. *Science* **290**, 1947–1951 (2000).
41. Steig, E. J. *et al.* Synchronous climate changes in Antarctica and the North Atlantic. *Science* **282**, 92–95 (1998).
42. Mulvaney, R. *et al.* The transition from the last glacial period in inland and near-coastal Antarctica. *Geophys. Res. Lett.* **27**, 2673–2676 (2000).
43. Kanfoush, S. L. *et al.* Millennial-scale instability of the Antarctic Ice Sheet during the last glaciation. *Science* **288**, 1815–1818 (2000).
44. Weaver, A. J., Saenko, O. A., Clark, P. U. & Mitrovica, J. X. Meltwater pulse 1A from Antarctica as a trigger of the Bölling-Allerød warm interval. *Science* **299**, 1709–1713 (2003).
45. Wunsch, C. Greenland-Antarctic phase relations and millennial time-scale climate fluctuations in the Greenland ice-cores. *Quat. Sci. Rev.* **22**, 1631–1646 (2003).
46. Roe, G. H. & Steig, E. J. Characterization of millennial-scale climate variability. *J. Clim.* **17**, 1929–1944 (2004).
47. Broecker, W. S. Thermohaline circulation, the Achilles heel of our climate system: Will man-made CO₂ upset the current balance? *Science* **278**, 1582–1588 (1997).
48. Timmermann, A., Justino, F. B. & Jin, F.-F. Surface temperature control in the north and tropical Pacific during the last glacial maximum. *Clim. Dyn.* (in the press).
49. IPCC. *Climate Change: The Scientific Basis. Contribution of Working Group I to the Third Assessment Report of the Intergovernmental Panel on Climate Change* (Cambridge Univ. Press, Cambridge/New York, 2001).
50. Enting, I. G. On the use of smoothing splines to filter CO₂ data. *J. Geophys. Res.* **92**, 10977–10984 (1987).

Supplementary Information accompanies the paper on www.nature.com/nature.

Acknowledgements We are grateful to the model developers and KNMI for making ECBILT-CLIO available to the scientific community, to F. Justino and U. Krebs for setting-up the glacial version of the model, and to N. Shackleton for discussions. This work was supported by the Swiss National Science Foundation, the Swiss Federal Office of Science and Education through the EC project POP and the University of Bern. A.T. was supported by the Deutsche Forschungsgemeinschaft through a Collaborative Research Project.

Competing interests statement The authors declare that they have no competing financial interests.

Correspondence and requests for materials should be addressed to R.K. (knutti@climate.unibe.ch).